Quantification of optical attenuation coefficient based on continuous wavelet transform of photoacoustic signals measured by a focused broadband acoustic sensor

T. Hirasawa*[a], S. Okawa [a], M. Fujita [b], T, Kushibiki [a], M. Ishihara [a]
[a] Department of Medical Engineering, National Defense Medical College, 3-2 Namiki, Tokorozawa, Saitama, Japan;
[b] Second Division, Aeromedical Laboratory, Japan Air Self-Defense Force, 1-2-10 Sakae, Tachikawa, Tokyo, Japan;

ABSTRACT

We proposed a method of quantifying the effective attenuation coefficients of optical absorbers which uses the continuous wavelet transform to calculate the time-resolved frequency spectra of photoacoustic (PA) signals. In order to apply the method to blood oxygenation monitoring of blood vessels, this study discusses how to reduce the effects of blood vessel diameters, which influences on the time resolved frequency spectra of PA signals. Numerical simulations which calculate the PA signals produced from blood vessel phantoms with various diameters were performed. The simulations revealed that the frequency of PA signal became independent from the vessel diameters by measuring the PA signal from small area. The frequencies of simulated PA signals were proportional to the effective attenuation coefficients with a correlation coefficient of 0.99, and a slope of 0.035 MHz/cm^{-1} under condition that the measurement area was 4.0 mm at a frequency of 1.5 MHz. Thus we used the focused acoustic sensor of which focusing the foregoing measurement area. It consisted of a P(VDF-TrFE) film, which was characterized by broad frequency band. As results of experiments using the focused acoustic sensor, the frequencies of PA signals produced from blood vessel phantoms were proportional to the effective attenuation coefficients with correlation coefficient of 0.96 although the frequencies were suffered from deviations of 0.135 MHz, which corresponded to the effective attenuation coefficient of 3.46 cm^{-1}. Since the large deviations were caused by experimental factors such as sensor alignment, it is required to improve robustness to the experimental factors.

Keywords: Effective attenuation coefficient, Optical absorption coefficient, Functional monitoring, Blood oxygen saturation, Blood gas monitoring, Frequency analysis

1. INTRODUCTION

Photoacoustic imaging (PAI) technique is based on the generation of photoacoustic (PA) pressure waves, which generate ultrasound waves when optical absorbers absorb excitation light – generally, pulsed laser beams that satisfy thermal and stress confinement requirements [1]. These PA pressure waves propagate through biological tissues and can be measured as PA signals by acoustic sensors. PAI technique offers the spatial mapping of optical absorbers by calculating the distance between the acoustic sensors and optical absorbers from time delays of PA signals detection from the laser excitation time.

Optical absorption provides the dominant contrast in PAI, because intensities of PA signals produced by optical absorbers are generally proportional to amount of optical energies absorbed by the optical absorbers. Optical absorption coefficients of optical absorbers strongly depend on optical wavelengths. Since the dependences called optical absorption spectra varies with kinds of optical absorbers, PA images obtained at multiple optical wavelengths enable to determine the kinds of optical absorbers. The spectroscopic techniques called spectroscopic photoacoustic (sPA) [2] and other similar techniques [3] have been used to detect lipids in arterial wall [4], identify melanomas [5], and image exogenous contrast agents [6-9]. The techniques also enable to quantify the blood oxygen saturation by resolving deoxy-hemoglobin and oxy-hemoglobin in blood. Measuring the blood oxygen saturation in this manner has the advantages of higher spatial resolution and non-invasiveness compared to conventional methods such as pulse oximetry or gas analysis. To calculate the blood oxygen saturation from PA signals, the optical absorption coefficient or the effective attenuation coefficient of the blood should be quantified at each excitation wavelength. To quantify the coefficients, it is necessary to take account

* Takeshi Hirasawa : E-mail : hirasawa@ndmc.ac.jp, Telephone : +81 4 2995 1596

Photons Plus Ultrasound: Imaging and Sensing 2014, edited by Alexander A. Oraevsky, Lihong V. Wang,
Proc. of SPIE Vol. 8943, 89435Z · © 2014 SPIE · CCC code: 1605-7422/14/$18 · doi: 10.1117/12.2041676

of the optical energy densities (fluences) on optical absorber surfaces which also affect PA signals. Owingto strong optical scattering in biological tissues, however, the fluences on optical absorber surfaces are usually unknown. Thus, considerable attentions have been paid to developing methods for quantifying the coefficients [10].

Intensities of PA signals that proportional to amounts of optical energies absorbed by optical absorbers are used to quantify the optical absorption coefficients of the optical absorbers. Amounts of optical energies absorbed by the optical absorbers can be calculated as products of the optical absorption coefficients and the fluences on the optical absorber surfaces. Thus, the relative values of the optical absorption coefficients can usually be obtained by accounting for the fluences on the optical absorber surfaces. Model based techniques are proposed to quantify the coefficients. The techniques solve an inverse problem of the PA wave equation combined with the radiative transfer equation [11]. However, the techniques typically involve a computationally intensive iterative algorithm, making it difficult to quantify the optical absorption coefficients in real time.

To overcome these barriers, PA signal waveforms that depend on depth profiles of absorbed optical energies are used to quantify effective attenuation coefficients of optical absorbers [12-14]. Because optical energy attenuates exponentially along the light transfer axis in an optical absorber, PA signal waveforms detected along the light transport axis will have exponentially attenuated forms. Thus, the coefficients can be quantified by fitting the temporal waveforms to the exponential attenuation functions. One major advantage of the method is that the coefficients can be quantified on the basis of the relative temporal attenuation profiles of the PA signals, making it unnecessary to determine the fluences on the optical absorber surfaces. However, to quantify the accurate values of the coefficients, the PA signals should be measured by in two limited detection modes: near-field detection, in which the PA signals can be considered to be plane waves [13], and forward mode detection, in which the sample is irradiated by an excitation light source located on the far side of the acoustic sensor [12, 14]. Neither of these, however, is considered appropriate for measuring deep regions of thick biological tissue.

PA signal frequency spectra have also been used to derive the effective attenuation coefficients of optical absorbers [15]. The frequency spectra efficiently extract features of the PA signal waveforms. Because PA signals are unsteady pulsed waves, they have time varying frequency content; however, as the Fourier transform has no time resolution, only the time averaged frequency spectra are calculated. This blurs the temporal change of the frequency contents of the PA signals. Thus, we proposed the method to quantify effective attenuation coefficients which uses continuous wavelet transform (CWT) to calculate time-resolved frequency spectra from PA signal waveforms [16-18]. In the method, the maximum value of the dominant frequency calculated from time resolved frequency spectra was used to quantify the coefficient. We have already demonstrated that the frequency enable to quantify the coefficient using the planar optical absorber placed in transparent medium.

In this study, we discussed the application of the method to oxygen saturation monitoring of blood vessels. The application requires quantifying the effective attenuation coefficients independently from blood vessel diameters. However, the time resolved frequency spectra of PA signals were affected by geometries of optical absorbers. To reduce effects of blood vessel diameters onto PA signals, we proposed to detect PA signals from small area. Numerical simulations were performed using blood vessel phantoms with various diameters. Furthermore, we performed experiments using a focused acoustic sensor to detect PA signals from small area. To measure the broadband frequency contents of PA signals, the focused acoustic sensor made of P(VDF-TrFE) was used.

2. MATHERIAL AND METHOD

2.1 Continuous wavelet analysis of PA signals

The CWT is a spectral analysis method that can produce time-resolved frequency spectra of PA signals. The CWT modulus $T(a,b)$ is defined as the convolution of the temporal signal $p(t)$ and the dilated and temporally translated version of a wavelet function $\Psi(t)$ [19, 20]:

$$T(a,b)=a^{-\frac{1}{2}}\int_{-\infty}^{\infty}p(t)\Psi^{*}\left(\frac{t-b}{a}\right)dt, \qquad (1)$$

where $\Psi^{*}(t)$ is the complex conjugate of $\Psi(t)$, a is the dilation parameter, and b is the location parameter. Here, the complex Morlet wavelet, which is defined as a complex sinusoid with a Gaussian envelope, is used [19]:

$$\Psi(t) = \pi^{-\frac{1}{4}} \left(e^{-i\omega_0 t} - e^{-\omega_0^2 t} \right) e^{-\frac{t^2}{2}}, \qquad (2)$$

where ω_0 is central frequency of the wavelet, which determines number of sinusoidal waves within the Gaussian envelope. The dilation parameter a can be transformed into the frequency f using the equation $f = \omega_0/a$, where the time t replaces the location parameter b. Thus, the CWT produces time-resolved frequency spectra $T(f, t) = T(\omega_0/a, b)$ with a power given by $|T(f, t)|^2 = \mathrm{Re}[T(f, t)]^2 + \mathrm{Im}[T(f, t)]^2$.

The dominant frequencies of PA signals at each time points were calculated as the frequencies satisfying $d|T(f, t)|^2/df = 0$. The maximum value of the dominant frequency were calculated to quantify effective attenuation coefficients of optical absorbers [18].

2.2 Numerical simulation

To verify effects of vessel diameters onto maximum dominant frequencies of PA signals, PA signals produced from blood vessel phantoms with various diameters immersed in turbid medium were calculated by simulating both light transport and ultrasound propagation.

Figure 1(a) shows the geometry used in the numerical simulation. Blood vessel phantoms with wall thicknesses of 1 mm and inner diameters of 4.0, 5.0, and 6.0 mm were placed in a turbid medium. The tube phantoms were filled with six optical absorbers with different effective attenuation coefficients. The upper surface of the optical absorber was placed 8 mm away from the turbid medium surface. The optical properties of both turbid medium and optical absorbers were shown in Table 1. Both the reduced scattering coefficient and the optical absorption coefficient of the turbid medium correspond to that of typical biological tissues at NIR wavelength [21]. The coefficients of the optical absorbers corresponds to that of blood with an oxygen saturation of 0% to 100% at a wavelength of 756 nm [12, 22]. The acoustic sensor was contacted to the turbid media surface via 12 mm thick transparent medium.

The three-dimensional Monte Carlo light dosimetry software (3dgpu) developed by Lo and Lilge was used to simulate light transport in turbid medium [23]. The volume 15 x 15 x 25 mm within the turbid media was discretized into 300 x 300 x 500 voxels with sizes of 50 x 50 x 50 μm in x, y, and z directions. Propagation of 2 billion photon packets irradiated from top surface of the turbid medium were simulated to calculate the spatial distribution of absorbed optical energy $A(x, y, z)$.

PA signals produced from the blood vessel phantoms were calculated by solving PA wave equation. Assuming that the laser pulse widths are much shorter than the thermal diffusion time in the optical absorber and that acoustic inhomogeneity and viscosity of the medium are negligible, the PA wave equation can be given as [1]:

$$c^2 \nabla^2 p(\mathbf{r}, t) - \frac{\partial^2 p(\mathbf{r}, t)}{\partial t^2} = \frac{\beta c^2}{C_p} \frac{\partial H(\mathbf{r}, t)}{\partial t}, \qquad (1)$$

where c is speed of sound in the medium, β is the isobaric volume expansion coefficient, C_p is the specific heat, $p(\mathbf{r}, t)$ is PA pressure wave, and $H(\mathbf{r}, t)$ is the heat energy generated by optical absorption. The heat energy $H(\mathbf{r}, t)$ can be expressed as the product of the spatial distribution of the absorbed optical energy $A(\mathbf{r})$ and the temporal waveform of the laser pulse $\eta(t)$. The solution to Eq. 1 in the time domain can generally be expressed as [14, 18]:

$$p(\mathbf{r}', t) = \frac{\beta}{4\pi C_p} \left(\frac{1}{t} \iint_{|\mathbf{r}-\mathbf{r}'|=ct} A(\mathbf{r}-\mathbf{r}')\, dS \right) * \eta'(t) \qquad (2)$$

where $\mathbf{r}'$ is an observation point. The spatial distribution of absorbed optical energies $A(x, y, z)$ calculated by the light transport simulation was substituted into the Eq. 2. PA signals detected by a coaxial focused acoustic sensor with outer diameter of 6.0mm, inner diameter of 2.3 mm, and focal length of 25 mm were calculated. The dimension of the sensor was taken into accounted by performing a surface integration process in which the sensor was discretized into 3600 elements and then the PA signals detected by each element were calculated using Eq. 2. Finally, the individual signals were numerically integrated in order to calculate the total PA signal detected by the sensor surface. The measurement area of the sensor was 4.0 mm at a frequency of 1.5 MHz.

Time resolution of the entire simulation was limited by both voxel size of the light transport simulation and the time increment of the ultrasound propagation simulation. The voxel size of light transport simulation limits the time resolution

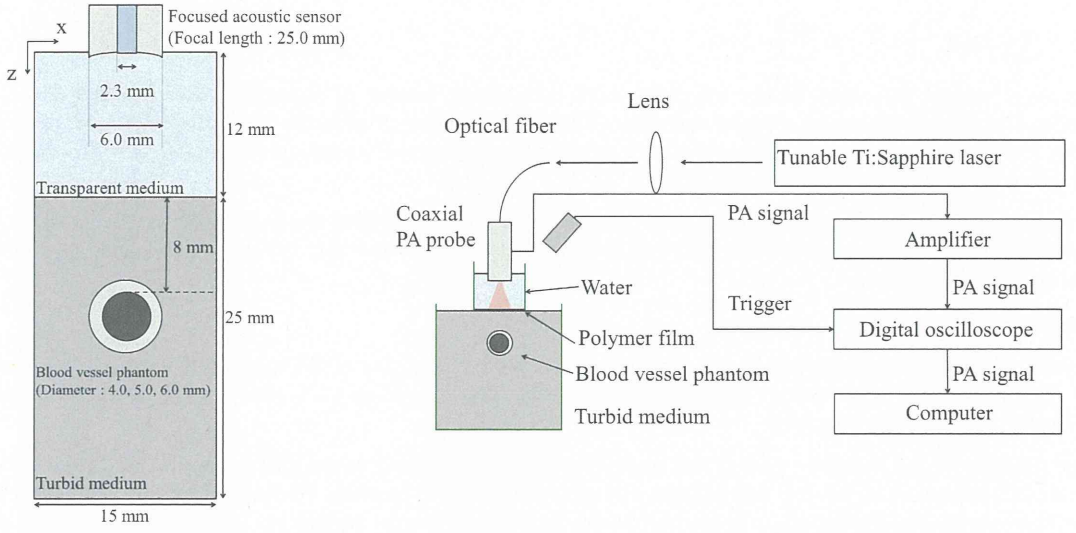

Fig.1 (a) Geometry used in numerical simulation, (b) Schematic diagram of experimental setup

Table 1 Optical properties of optical absorbers and a turbid medium used in both experiment and numerical simulation

Location	μ_a (cm^{-1})	μ_s' (cm^{-1})	μ_{eff} (cm^{-1})	μ_s (cm^{-1})	g
Absorber 1	8.36	25.5	29.1	75.4	0.662
Absorber 2	7.29	25.5	26.8	75.4	0.662
Absorber 3	6.22	25.5	24.3	75.4	0.662
Absorber 4	5.15	25.5	21.8	75.4	0.662
Absorber 5	4.08	25.5	19.0	75.4	0.662
Absorber 6	3.01	25.5	16.0	75.4	0.662
Turbid medium	0.10	10.0	1.74	29.6	0.662

by the ultrasound propagation time within a voxel. The propagation time 57.7 ns was calculated by dividing the diagonal length of the voxels 86.6 μm by the sound speed 1500 m/s. Since the time increment of ultrasound propagation simulation 10 ns was smaller than 57.7 ns, the time resolution of the entire simulation was 57.7 ns. Therefore, the Nyquist frequency of the entire simulation was 8.66 MHz.

2.3 Experiment using phantoms

To experimentally verify the effect of vessel diameters onto the dominant frequencies of PA signals, we measured PA signals produced from blood vessel phantoms with various diameters and effective attenuation coefficients.

A reflection mode PA measurement system was used to measure PA signals produced from blood vessel phantom. In the reflection mode system, the excitation light irradiation and PA signal detection occur on the same side of the sample [18]. The schematic diagram of the experimental system is shown in Fig. 1(b). A tunable Ti:sapphire laser (LT-2211, Lotis Tii, Minsk, Belarus) pumped by the second harmonic of a Q-switched Nd:YAG laser (LS-2134, Lotis Tii, Minsk, Belarus) was used to produce excitation light pulses with a width of 10 ns and a repetition frequency of 15 Hz at a wavelength of 756 nm. The excitation light pulses were then coupled into a multi-mode optical fiber with a core diameter of 0.6 mm (M41L02, Thorlabs, Newton, NJ). The optical fiber was arranged coaxially relative to a specially designed ring-shape focused acoustic sensor. The focused acoustic sensor has ring-shape concave detection surface with focal

length of 25 mm, outer diameter of 6.0 mm and inner diameter of 2.3 mm. The acoustic sensor was fabricated from a 20 μm-thick piezoelectric film P(VDF-TrFE) (KF piezo-film, Kureha Corp., Tokyo, Japan), which has a wider frequency bandwidth than that of a lead zirconium titanate piezoelectric ceramic. The PA signal detected by the acoustic sensor was amplified by a low noise field-effect transistor amplifier (SA-220F5, NF Electronic Instruments, Yokohama, Japan) and then recorded by a digital oscilloscope (M9210A, Agilent Technology, Santa Clara, CA) with a sampling rate of 2 GSa/s, and a bit depth of 12 bit.

Low-density polyethylene (LDPE) tubes (T0310, Yamaichi Chemical, Osaka, Japan) with wall thickness of 1.0 mm and inner diameters of 4.0, 5.0, and 6.0 mm filled with optical absorbers were used as blood vessel phantoms. The blood vessel phantoms were immersed in the turbid medium at a depth of 8.0 mm from the turbid medium surface. Mixtures of specific black ink (Black Ink, Pilot, Tokyo, Japan) and intralipid (Intralipid fluid solution 20 %, Fresenius Kabi AB, Germany) were used as optical absorbers and a turbid media. Optical properties of optical absorbers and a turbid media were shown in Table 1. To place the tube phantoms at focal zone of the focused acoustic sensor, we used the degassed water filled in small water tank as an acoustic spacer. The bottom of the small water tank was an 11 μm-thick clear polymer film selected to ensure minimal attenuation of excitation light pulses and PA signals. The bottom of the water tank was on the ambient medium surface. The acoustic sensor was immersed in the degassed water and placed 20 mm away from the tube phantoms. The experiment was performed with excitation pulse energy of 4.0 mJ.

3. RESULTS AND DISCUSSION

3.1 Numerical simulation

A spatial distribution of absorbed optical energies calculated by the light transport simulation is shown in Fig. 2(a). The surface of the turbid medium was z = 12 mm. The top surface of a blood vessel phantom with a diameter of 6 mm and an effective attenuation coefficient of 29.1 cm^{-1} was z = 20 mm. The excitation light irradiated from the top surface of the turbid medium was absorbed by both the turbid medium and the blood vessel phantom.

A simulated PA signal measured by the focused acoustic sensor is shown in Fig. 2(b). PA signals produced from the turbid medium and the tube phantoms were observed at t = 8 μs and 13.3μs, respectively. Figure 3(a) shows the CWT of the PA signal observed at 12 - 16 μs. Two maxima observed in the CWT originate from the positive and the negative peaks of the PA signal waveform, respectively. Figure 3(b) shows dominant frequencies of the PA signal as a function of time. The maximum of the dominant frequency observed at the positive peak of the PA signal was used to quantify the effective attenuation coefficient. Figure 4 shows the parameters as functions of the effective attenuation coefficients of the phantoms. The maximum of dominant frequencies obtained from the PA signals measured by focused acoustic sensor were proportional the effective attenuation coefficient with a correlation coefficient of 0.99, and a slope of 0.035

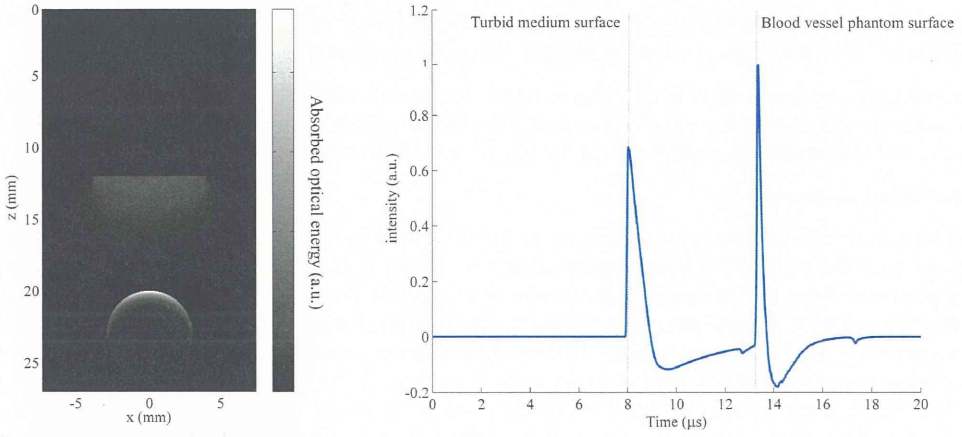

(a) (b)

Fig. 2 (a) Example of simulated spatial distribution of absorbed optical energies and (b) simulated PA signals measured by focused acoustic sensor (b)

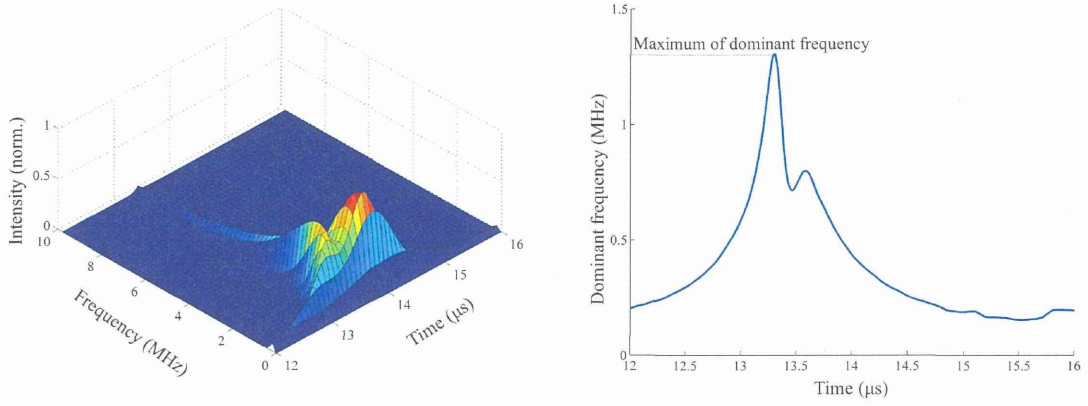

(a) (b)

Fig. 3 (a) CWT of the simulated PA signal (b) dominant frequencies of the PA signal calculated from CWT as a function of time.

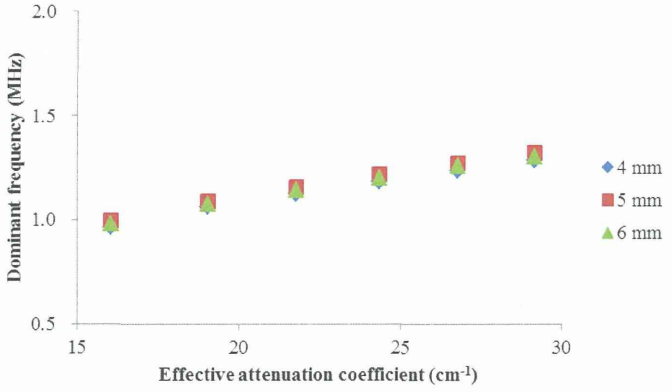

Fig.4 Maximum of the dominant frequencies of simulated PA signals produced from blood vessel phantoms with various diameters as functions of effective attenuation coefficients of optical absorbers.

MHz/cm^{-1}. Additionally, the frequencies were independent of the blood vessel diameters. These results suggest that the maximum dominant frequencies of PA signals produced from blood vessels enable to quantify the effective attenuation coefficients of the blood vessels independently from the blood vessel diameters.

3.2 Experiment using phantoms

PA signals produced from blood vessel phantoms were measured by the focused acoustic sensor. To calculate maximum dominant frequencies, CWTs of the PA signals were calculated. Figure 5 shows the maximum dominant frequencies of the PA signals produced from the phantoms with various diameters as functions of effective attenuation coefficients. Although the frequencies were proportional to the effective attenuation coefficients with correlation coefficient of 0.96, the measured values shown in Fig. 5 were slightly different from the simulated values shown in Fig. 4. This difference is caused by frequency response of the focused acoustic sensor. By convolving the frequency response of the sensor into the simulated PA signal, these results will match. The frequencies shown in Fig. 4 were suffered from deviations of 0.135 MHz. The deviation was caused by slight change of the sensor angle and position. Since slight change of the sensor alignment displaces the sensitive region of the sensor, the sensor measures PA signals produced at different area of the optical absorber. The optical absorber surface within the sensitive area of the sensor strongly affects the frequency of PA signal, because the optical absorber surfaces strongly absorb excitation light. Thus, change of the optical absorber

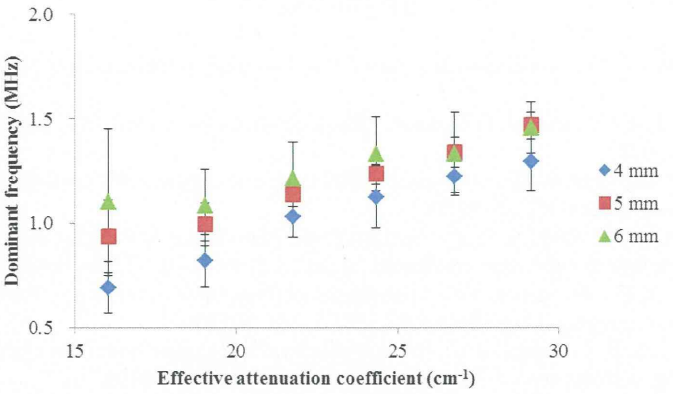

Fig.5 Dominant frequencies of PA signals produced from blood vessel pahntom with various diameters as a function of effective attenuation coefficient (error bar: standard deviation, n=3).

surface within the sensitive region of the sensor due to the slight change of alignment causes the frequency change of PA signals. Since the blood vessel phantom with small diameter have small curvature radius, the PA signal produced from phantoms with small diameters were sensitive to the alignment of the sensitive region of the sensor. Thus, it is necessary to improve robustness to experimental factors such as sensor alignment. In order to reduce the frequency change, the sensitive region of focused acoustic sensor should be sufficiently narrower than the blood vessel diameter. The narrower sensitive region can be obtained by increasing the numerical apertures of focused acoustic sensors. Another approach is extract other parameters from CWTs of PA signals to correct the frequency changes.

4. CONCLUSION

In this paper, we discussed the application of the method of quantifying the effective attenuation coefficients to blood oxygenation monitoring of blood vessels. The method uses the continuous wavelet transform to calculate the time-resolved frequency spectra of photoacoustic (PA) signals. The time resolved frequency spectra of PA signals were affected by geometries of optical absorbers. Numerical simulations of a light transport and ultrasound propagation were performed to calculate temporal waveforms of PA signals produced from blood vessel phantoms with various diameters and optical properties placed in the turbid medium. As results of simulations, by measuring the PA signal from small area, the maximum dominant frequencies of the PA signals calculated by using the CWT were proportional to the effective attenuation coefficient with a correlation coefficient of 0.99, and a slope of 0.035 MHz/cm^{-1}, and the frequencies were independent of the tube diameter. The simulation result suggested that the frequencies of PA signals measured from small area enable to quantify the effective attenuation coefficient of the blood in the blood vessels with various diameters. We also performed experiment using blood vessel phantoms with various diameters. In the experiment, to measure the PA signals from small area, the focused acoustic sensor made of P(VDF-TrFE) was used. As results of the experiments, the maximum dominant frequencies of PA signals calculated from CWTs of the PA signals were proportional to the effective attenuation coefficients of blood vessel phantoms. However, the frequencies were suffered from large deviations of 0.135 MHz. The deviation was caused by slight difference of the sensor alignment because the frequencies of PA signals produced from phantoms with small diameters are sensitive to the sensor alignment. Thus, it is necessary to improve robustness to experimental factors such as sensor alignment. Use of a focused acoustic sensor with higher numerical aperture will enable to reduce the effect of experimental factors such as sensor alignment.

ACKNOWLEDGMENT

This research was partially supported by JSPS KAKENHI Grant Number 25750192 and 25282158, a Health and Labor Science Research Grant for Research on Medical Device Development, and JST Collaborative Research Based on Industrial Demand (In vivo Molecular Imaging : Towards Biophotonics Innovations in Medicine). The authors appreciate the contributions of Mr. Y. Ikeda, and Mr. H. Ishihara to this study. Experiments were supported by the Laboratory Center, National Defense Medical College.

REFERENCES

[1] C. Li, and L. V. Wang, "Photoacoustic tomography and sensing in biomedicine," Phys Med Biol, 54(19), R59-97 (2009).

[2] S. Y. Emelianov, P.-C. Li, and M. O'Donnell, "Photoacoustics for molecular imaging and therapy," Physics today, 62(8), 34 (2009).

[3] A. Taruttis, M. Wildgruber, K. Kosanke *et al.*, "Multispectral optoacoustic tomography of myocardial infarction," Photoacoustics, 1(1), 3-8 (2013).

[4] T. J. Allen, A. Hall, A. P. Dhillon *et al.*, "Spectroscopic photoacoustic imaging of lipid-rich plaques in the human aorta in the 740 to 1400 nm wavelength range," J Biomed Opt, 17(6), 061209-1-061209-10 (2012).

[5] H. F. Zhang, K. Maslov, G. Stoica *et al.*, "Functional photoacoustic microscopy for high-resolution and noninvasive in vivo imaging," Nat Biotechnol, 24(7), 848-51 (2006).

[6] A. d. l. Zerda, Z. Liu, S. Bodapati *et al.*, "Ultrahigh sensitivity carbon nanotube agents for photoacoustic molecular imaging in living mice," Nano letters, 10(6), 2168-2172 (2010).

[7] G. P. Luke, D. Yeager, and S. Y. Emelianov, "Biomedical Applications of Photoacoustic Imaging with Exogenous Contrast Agents," Annals of biomedical engineering, 1-16 (2012).

[8] I. Y. Petrov, Y. Petrov, D. S. Prough *et al.*, "Optoacoustic monitoring of cerebral venous blood oxygenation through extracerebral blood," Biomed Opt Express, 3(1), 125-36 (2012).

[9] H. F. Zhang, K. Maslov, M. Sivaramakrishnan *et al.*, "Imaging of hemoglobin oxygen saturation variations in single vessels in vivo using photoacoustic microscopy," Appl Phys Lett, 90(5), 053901-053901-3 (2007).

[10] B. Cox, J. G. Laufer, S. R. Arridge *et al.*, "Quantitative spectroscopic photoacoustic imaging: a review," J Biomed Opt, 17(6), 061202 (2012).

[11] J. Laufer, B. Cox, E. Zhang *et al.*, "Quantitative determination of chromophore concentrations from 2D photoacoustic images using a nonlinear model-based inversion scheme," Appl Opt, 49(8), 1219-1233 (2010).

[12] J. Laufer, C. Elwell, D. Delpy *et al.*, "In vitro measurements of absolute blood oxygen saturation using pulsed near-infrared photoacoustic spectroscopy: accuracy and resolution," Phys Med Biol, 50, 4409-4428 (2005).

[13] M. Jaeger, M. Hejazi, and M. Frenz, "Diffraction-free acoustic detection for optoacoustic depth profiling of tissue using an optically transparent polyvinylidene fluoride pressure transducer operated in backward and forward mode," J Biomed Opt, 10(2), 024035-024035-7 (2005).

[14] Y. Wang, and R. Wang, "Photoacoustic recovery of an absolute optical absorption coefficient with an exact solution of a wave equation," Phys Med Biol, 53(21), 6167-77 (2008).

[15] Z. Guo, C. Favazza, A. Garcia-Uribe *et al.*, "Quantitative photoacoustic microscopy of optical absorption coefficients from acoustic spectra in the optical diffusive regime," J Biomed Opt, 17(6), 066011 (2012).

[16] T. Hirasawa, M. Fujita, S. Okawa *et al.*, "Improvement in quantifying optical absorption coefficients based on continuous wavelet-transform by correcting distortions in temporal photoacoustic waveforms," Proc. of SPIE, 8581, 85814J (2013).

[17] T. Hirasawa, M. Ishihara, K. Tsujita *et al.*, "Continuous wavelet-transform analysis of photoacoustic signal waveform to determine optical absorption coefficient," Proc. of SPIE, 8223, 822333 (2012).

[18] T. Hirasawa, M. Fujita, S. Okawa *et al.*, "Quantification of effective attenuation coefficients using continuous wavelet transform of photoacoustic signals," Appl Opt, 52(35), 8562-8571 (2013).

[19] P. Addison, J. Watson, and T. Feng, "Low-oscillation complex wavelets," Journal of Sound and Vibration, 254(4), 733-762 (2002).

[20] P. Addison, [The illustrated wavelet transform handbook: introductory theory and applications in science, engineering, medicine] London: Institute of Physics Publishing, (2002).

[21] L. V. Wang, and H.-i. Wu, [Biomedical optics: principles and imaging] John Wiley and Sons, Hoboken, NJ(2007).

[22] S. L. Jacques, and S. A. Prahl, [Absorption Spectra for Biological Tissues (Oregon Medical Laser Center, OR)], (2004).

[23] W. C. Y. Lo, and L. Lilge, "Accelerated 3D Monte Carlo light dosimetry using a graphics processing unit (GPU) cluster," Proc. of SPIE, 737609 (2010).

Quantification of effective attenuation coefficients using continuous wavelet transform of photoacoustic signals

Takeshi Hirasawa,[1,*] Masanori Fujita,[2] Shinpei Okawa,[1]
Toshihiro Kushibiki,[1] and Miya Ishihara[1]

[1]Department of Medical Engineering, National Defense Medical College, 3-2, Namiki, Tokorozawa, Saitama 359-8513, Japan

[2]Division of Environmental Medicine, National Defense Medical College Research Institute, 3-2, Namiki, Tokorozawa, Saitama 359-8513, Japan

*Corresponding author: hirasawa@ndmc.ac.jp

Received 11 July 2013; revised 8 November 2013; accepted 13 November 2013; posted 14 November 2013 (Doc. ID 193028); published 6 December 2013

A method for quantifying the effective attenuation coefficients of optical absorbers by using the continuous wavelet transform (CWT) to calculate the time-resolved frequency spectra of photoacoustic signals is proposed. Because the coefficients can be quantified according to the relative intensity of the frequency content of the signals, it is unnecessary to determine the fluences. A computational simulation reveals that the time-resolved frequency spectra exhibit better correlation with the coefficients than do power spectra calculated using a Fourier transformation. The CWT-based method was experimentally verified, and the coefficients were quantified with mean square error of 2.0 cm^{-1}. © 2013 Optical Society of America

OCIS codes: (170.0110) Imaging systems; (170.1460) Blood gas monitoring; (170.2655) Functional monitoring and imaging; (170.5120) Photoacoustic imaging; (170.6935) Tissue characterization.
http://dx.doi.org/10.1364/AO.52.008562

1. Introduction

Photoacoustic imaging (PAI) is a combined ultrasound and optical imaging technique that allows for spatial mapping of optical absorbers in biological tissues. The PAI technique is based on the generation of photoacoustic (PA) pressure waves, which generate ultrasound waves when the optical absorber material absorbs excitation light—generally, pulsed laser beams that satisfy thermal and stress confinement requirements. These PA pressure waves propagate through biological tissues and can be measured as PA signals by acoustic sensors. By calculating the distances between the acoustic sensors and the optical absorbers using the speed of sound in the biological tissues and the time delay from the laser excitation time, a spatial mapping of the optical absorbers can be obtained.

Because oxy-hemoglobin and deoxy-hemoglobin are dominant optical absorbers in biological tissues at wavelengths of 700–900 nm, both produce strong PA signals over this wavelength range, which serves as an optical window that allows light to penetrate up to several centimeters into biological tissues [1]. Oxy-hemoglobin and deoxy-hemoglobin are know to have different optical absorption spectra [2–4], so PA signals measured at multiple excitation wavelengths can be used to distinguish between the two [5]; accordingly, measurement of PA signals can be used to determine the blood oxygen saturation, or the ratio of oxy-hemoglobin to total hemoglobin.

1559-128X/13/358562-10$15.00/0

Measuring the blood oxygen saturation in this manner has the advantages of higher spatial resolution and noninvasiveness compared to conventional methods such as pulse oximetry or gas analysis [6]. To calculate the blood oxygen saturation from PA signals, the optical absorption coefficient or effective attenuation coefficient of blood should be quantified at each excitation wavelength [3]. Considerable attention has been paid to developing methods for quantifying the values of these coefficients in optical absorbers [3,7–9]. The effective attenuation coefficient μ_{eff} can be expressed as follows:

$$\mu_{\text{eff}} = \{3\mu_a(\mu_a + \mu_s')\}^{\frac{1}{2}}, \quad (1)$$

where μ_s' is the reduced optical scattering coefficient, and μ_a is the optical absorption coefficient. Because the optical energy densities (fluences) affect PA signals, it is necessary to remove their effects in order to quantify the optical absorption coefficients or effective attenuation coefficients of optical absorbers [7].

The amplitude of a PA signal can be calculated as the product of the optical absorption coefficient, the fluence on the surface of the absorber, and a proportional factor called the Grüneisen parameter, which expresses the efficiency of conversion from heat to ultrasound energy. Because the Grüneisen parameter is assumed to be constant in most cases [3], the optical absorption coefficient can usually be calculated by dividing the PA signal amplitude by the product of the optical absorber surface fluence and the Grüneisen parameter. Owing to the strong optical scattering in biological tissues, however, the fluence on the surface of the optical absorber is usually unknown. One method for quantifying the optical absorption coefficient is to solve the radiative transfer equation and the PA wave equation [10]. However, the methods used to solve these equations typically involve a computationally intensive iterative algorithm, making it difficult to quantify the coefficient in real time.

To overcome these barriers, temporal PA signal waveforms that depend on the depth profiles of the absorbed optical energies [8,11,12] can be used to quantify the effective attenuation coefficients of optical absorbers. Because optical energy attenuates exponentially along the light transfer axis of an optical absorber, the temporal waveform of a PA signal detected along the light transport axis will have an exponentially attenuated form. One major advantage of the temporal waveform method is that the effective attenuation coefficients can be quantified on the basis of the relative temporal attenuation profiles of the PA signals, making it unnecessary to determine the fluences on the optical absorber surface. By using limited detection modes, the effective attenuation coefficients of an optical absorber can be quantified by fitting the temporal waveforms of PA signals to the exponential attenuation functions [10]. There are two limited detection modes: near-field detection, in which the PA signals can be considered to be plane waves [11,12], and forward-mode detection, in which the sample is irradiated by an excitation light source located on the far side of the acoustic sensor [3]. Neither of these, however, is considered appropriate for measuring deep regions of thick biological tissue.

PA signal frequency spectra have also been used to derive the effective attenuation coefficients of optical absorbers [9,13]. Frequency spectra, which are generally calculated using the Fourier transform (FT), efficiently extract the features of PA signal temporal waveforms. Because PA signals are unsteady pulsed waves, they have time-varying frequency content; however, as the FT has no time resolution, only the time-averaged frequency spectra are calculated. This blurs the temporal change of the frequency contents of the PA signals. Thus, frequency analysis of PA signals should employ time-resolved methods.

In this paper, we propose the use of the continuous wavelet transform (CWT) to calculate the time-resolved frequency spectra from the temporal waveforms of PA signals [14,15]. The CWT, which can produce time-resolved frequency spectra, is widely used to analyze unsteady signals with time-variable frequency content. Indeed, previous studies have already used the wavelet transform to reduce PA signal noise; for instance, Viator and others used the discrete wavelet transform to reduce white noise from PA signals [16–18], and Li *et al.* and others used CWT to calculate the band-pass filtered PA signal characteristics over various frequency ranges in order to determine which frequency band offers the maximum signal-to-noise ratio [19–21]. However, we could not find any studies in which the CWT was used for frequency analysis rather than noise reduction.

In this study, we analyzed the relationship between the time-resolved frequency spectra of PA signals and the effective attenuation coefficients of optical absorbers, as these correlations strongly affect the accuracy of quantification. We then calculated the coefficients of optical absorbers using the time-resolved frequency spectra of PA signals measured by our original PA measurement system [22]. Finally, these calculated values were compared with the values determined by two methods; one uses the frequency spectra of PA signals calculated using FT, and another uses the temporal waveform of the PA signals.

2. Theoretical Background

A. Detection of PA Signal

PA pressure waves consist of ultrasound energy packets produced by an optical absorber that has absorbed short laser pulses. Assuming that the laser pulsewidths are much shorter than the thermal diffusion time in the optical absorber and that the acoustic inhomogeneity and viscosity of the medium are negligible, the wave equation of the PA pressure $p(\mathbf{r}, t)$ (Nm^{-2}) can be given as [1,23]